PAPER • **OPEN ACCESS**

Numerical Study of Pre-Duct on Traditional Fishing Vessels as Energy Saving Device (ESD)

To cite this article: A Munazid *et al* 2020 *IOP Conf. Ser.: Earth Environ. Sci.* **557** 012049

Numerical Study of Pre-Duct on Traditional Fishing Vessels as Energy Saving Device (ESD)

A Munazid[1], I M Ariana[1], and I K A P Utama[2]

[1]Department of Marine Engineering, Institut Teknologi Sepuluh Nopember (ITS), Surabaya 60111, Indonesia.
[2]Department of Naval Architecture, Institut Teknologi Sepuluh Nopember (ITS), Surabaya 60111, Indonesia.

E-mail : alimunazid@gmail.com,

Abstract. This paper is aimed to investigate the effect of Energy Saving Device (ESD), namely Pre-Duct on traditional fishing vessels, in improving ship propulsor performance thus increase energy efficiency. Traditional fishing vessel in Lamongan coast are fishing vessels built by local shipbuilders based on experience and shipbuilder instincts from ancestors not based on the design of vessels, hull shape parametric of vessel is : $L/\nabla^{1/3}$=3.97; L/B=3.06; Cb=0.49; Cm=0.73; Cw=0.78; Cp=0.7 and principal particulars of traditional fishing vessel is : Loa=9.5 m; Bmld=3.10 m; H=1.2 m; T=0.95 m. Simulation study on traditional fishing vessels was conducted using CFD approach together with the use of CFX commercial code; the simulation results determined the thrust and propulsive coefficient of vessels with and without pre-duct. Based on systematic comparisons of pre-duct and without pre-duct on traditional fishing vessels, the implementation of pre-duct has increased efficiency of energy and improving ship propulsor performance about 3%.

1. Introduction

The operation of a main engine powered vessels with fossil fuel, produces emissions that have an impact on increasing air pollution into the atmosphere [1]. The impact of the increase in air pollution has become a crucial problem today, therefore serious action must be taken into consideration. Furthermore, the operational of vessels closely relate to both economic and environmental issues. Those issues have enforced naval architects to design and build vessels that have low emissions in one hand and maximize energy efficiency and lower operational cost of the vessels, in the other hand [2][3].

The increase in demand for energy savings due to the increase of fuel costs and the inconsistence on implementing stricter environmental regulations on some of the vessels types has become very important concerns for vessel-owners. Lower vessel operating costs and compliance with regulations issued by IMO for example the Energy Efficiency Design Index (EEDI) and Energy Efficiency Operation Index (EEOI) for ships used has become mandatory from economic and regulatory perspectives. As a consequence, interest in using Energy Saving Devices (ESD), for instance, has increased significantly, because it is an easier and relatively cheaper way to improve the overall thrust and efficiency of ships, especially in the case of retrofitting when carried out on the hull and engine installations.

Energy Saving Device (ESD) can increase energy efficiency by two methods: (1) a device that increases the efficiency of propulsive force and (2) additional power by utilizing renewale energy

sources [4]. ESD based on hydrodynamic principles is classified into three operating zones as shown in Figure 1: Zone I / pre-device, Zone II / main device and Zone III / post-device [5].

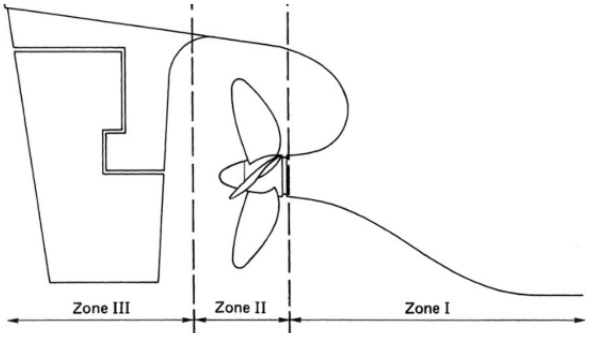

Figure 1. Zones for classification of energy-saving device [5]

The thrust of the vessels in generally influenced by the interaction of the hull, propeller and rudder blade, with optimizing the wake distribution, minimizing thrust deduction, recovery of rotating energy etc. This can be done by implementation of energy saving devices (ESD) such as pre-duct that are in Zone I / pre-devices. There are many implementation studies of pre-duct on large vessels with low speed, generally implementation pre-duct improve the performance of ship propulsion between 3-10%, [5][6][7][8][9][10].

Several developments of ESD type duct include: nozzle, stern duct, pre-duct [3], Mitsui Integrated Duct Propeller (MIDP) [4], Hitachi Zosen Nozzle (HZN) [5], Wake Equalizing Duct (WED)) [6] [7] [8] [9] [10], Sumitomo Integrated Lammeren Duct (SILD) [11] [12] [13], Semi-Circular Duct (Semi Duct) [14] [13], Backer Mewis Duct (Mewis Duct) [15] [16], Semi-Duct System with contra-Fins (SDS-F) [17], Blade Efficiency Improving Stator Duct (BSD) [18] [17]. Approach of Simulation Based Design Optimization (SBDO) [19] in order to reduce energy losses and reduce separation in after of the hull due to its flow acceleration effect. In addition, mass flux through the propeller increases, will increase ideal efficiency of propeller (reduce axial kinetic energy losses) which overall contributes positively to the efficiency, as well as increasing viscous wake capture through propeller disks and also increasing propeller and vessel interaction that contribute to efficiency, as explained by [2] and [20]. One of the benefit is increasing wake uniformity due to the effect of re-direction flow in the axial direction, which effectively reduces axial losses through changes in thrust distribution towards the hub (backward flow entering the propeller is more uniform), which changes to a uniform thrust distribution. Blade load is evenly distributed, meaning that slipstream is more uniform and lower kinetic losses in distant wakes and lower thrust deduction if the highest thrust reaches the hull (where the wake of the hull without ducts is slower) decreases, reducing blade section interaction with the hull ship.

The implementation of pre-duct technology on traditional fishing vessels to increased efficiency energy and improving ship propulsor performance, has become the current work focus in order to reduce fuel comsumption where the case study is conducted at Lamongan coastal area. For this reason, numerical (CFD) modeling of traditional fishing vessels with and without pre-duct is carried out to obtain the efficiency and performance of the ship propulsion system in each vessels.

2. Objective Vessel and Pre-Duct Design Concept

2.1. Traditional Fishing Vessel

Fishing vessel are floating facilities used by fishermen to catch and store fish [11]. Traditional fishing vessels on the Lamongan coast are fishing vessels built by local shipbuilders based on experience and shipbuilder instincts obtained from generation to generation from their ancestors and not based on the design of vessels [12][13][14]. Thus, the performance and characteristics of traditional fishing vessels are doubtful. The traditional fishing vessels of the Lamongan fishing community are traditionally built

vessels, the shape of the hull tends to be fat and shorts as shown in Figure 2, and particulars of vessel in Table 1.

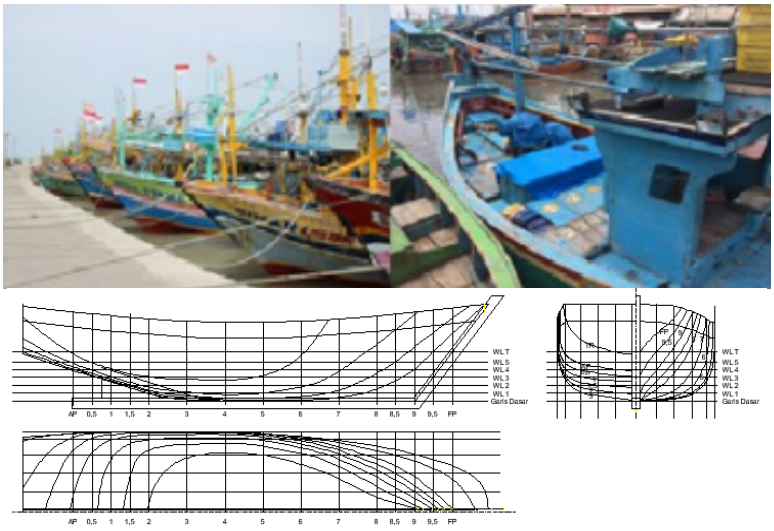

Figure 2. Traditional Fishing Vessels [13]

Table 1. Specification of Traditional Fishing Vessels

Particulars	Fishing Vessel	Unit
Length (Loa)	9,50	Meter
Breadth (Bmld)	3,10	Meter
Draft (T)	0,95	Meter
Coef. of Block (Cb)	0,49	--
Gross Tonnage (GT)	5,00	Tones
Speed Vessel (Vd)	6	Knot

2.2. Propeller

The propellers used as the main propulsion of traditional fishing vessels in Lamongan are using propellers of various shapes and sizes, most of the propellers that are used by the fishing community are traditional craftsmen and propeller factories. But it is unfortunate that the propeller is not equipped with clear information about the performance of the propellers used, the only information that can be obtained is the ratio of the diameter propeller and the number of blades propeller. One series of propellers that is often used and used on fishing vessels is the Wageningen propeller, better known as the B-Series propeller, as in Figure 3, and particulars as in Table 2.

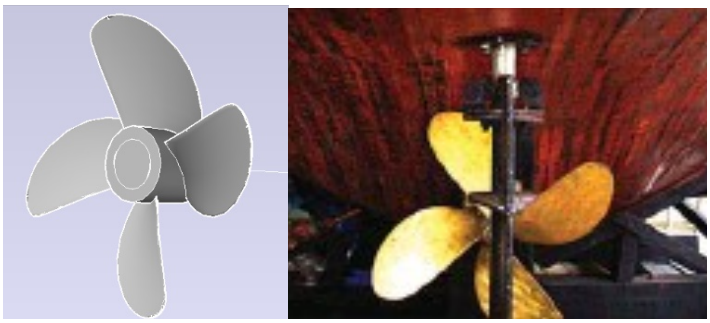

Figure 3. Propeller

Table 2. Specification of Propeller

Particulars	Propeller	Unit
Type	B4-40	--
Number of Blade	4	Blade
Rotation	412	Rpm
P/D	0,82	--
Diameter	275	mm

2.3. Pre-Duct Design Concept

Based on the basic principles of existing energy savings, the design concept of the pre-duct shape and location were used as follows: placing the pre-duct at a position where stern bilge vortices are strong, to recovery of surface pressure over stern hull and improvement of flow field at propeller plane with the straightening effect is enhanced. Thrust generation duct by placing the duct at a position where the angle of a diagonal flow is large which a forward thrust force of the duct is increased. Under these conditions the pre-duct is placed in Zone I ESD, which is in front of the propeller in the asymmetric form of the hydrofoil duct as shown in Figure 4.

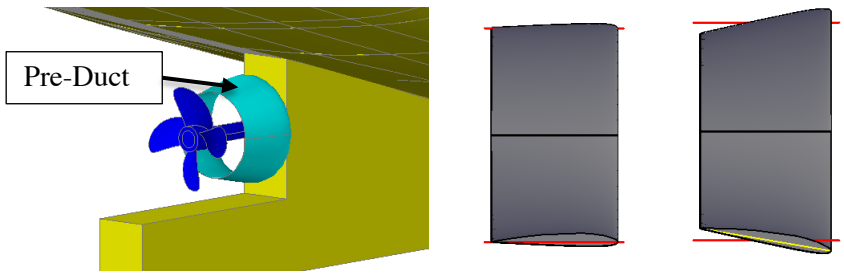

Figure 4. Pre-Duct Design

3. Method

3.1. Ship Propulsor

Interaction of the ship with water in forward motion, will experience a force that restrains forward motion, known as ship resistance, the magnitude of ship resistance must be able to be overcome by thrust generated by the ship's propulsion system. The components of the ship's propulsion system are: main engine unit, the transmission unit (shaft), and propeller. The concept of energy conversion of a ship propulsion system is to convert energy from fuel into thrust (T) in accordance with the ship's resistance (R) at a specified speed (V), as in Figure 5. The ship's propulsion system depends on: fuel (properties and quality); engine efficiency (the conversion of energy from fuel into poser produced) and propulsor efficiency (power conversion from propeller rotation into thrust generated), The

component of a ship's thrust include: the ship resistance in motion, propeller open water efficiency, interaction of the hull and propeller of the vessels [3][15], as illustrated in Figure 6.

Thrust efficiency which is a function of open water efficiency from propeller, hull efficiency and relative rotative efficiency, which indicated by Quasi-Propulsive Coefficient (QPC) [3],[15]. The quasi-propulsive coefficient relationship as in Equation (1).

$$\eta_D = \eta_0 \times \eta_H \times \eta_R \quad (1)$$

where η_D = Quasi propulsive coefficient, η_0 = Efficiency open water of propeller, η_H = Hull Efficiency, η_R = Relative rotative efficiency.

According to [3][16][17], component of propeller open water efficiency (η_0) is defined in Equation (2).

$$\eta_0 = \eta_a \times \eta_r \times \eta_f \quad (2)$$

where η_a: axial efficiency, η_r: losses due to fluid rotation caused by propellers, η_f: losses due to propeller blade friction resistance.

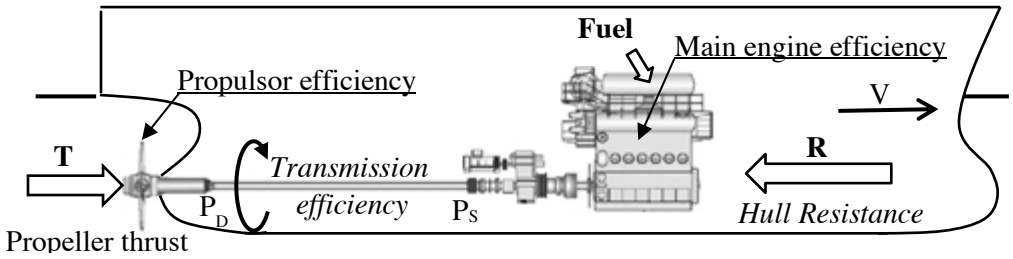

Figure 5. Concept of energy conversion in ship propulsion [15]

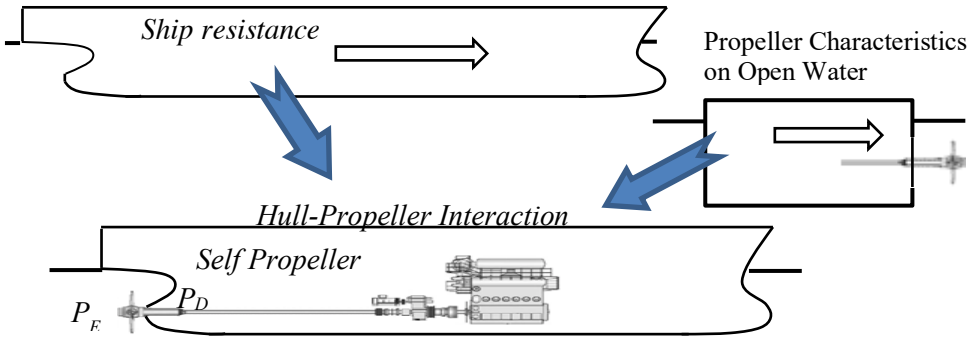

Figure 6. Component of ship propulsion [15]

The amount of propeller open water efficiency (η_0) depends on propeller parameters and operating conditions. Component investigation of open water conditions can use propeller blade momentum theory [3][18] as in Equation (3), (4) and (5).

$$\eta_a = \frac{1}{(1+a)} \quad (3)$$

$$\eta_r = (1 - a') \quad (4)$$

$$\eta_f = \frac{\tan\emptyset}{\tan(\emptyset+\gamma)} \quad (5)$$

where a and a' are axial and rotational inflow factors, from the momentum and correction of the number of propeller blade using the Goldstein correction factor [3].

Efficiency of hull (η_H) is the ratio of effective power (P_E) and thrust (P_T). The efficiency of hull (η_H) is between 1,0 – 1,25 for displacement vessels, in Equation (6), shows that the change in thrust deduction (t) is caused by steering several other object which overall affect the propeller efficiency, while the wake fraction (w).

$$\eta_H = \frac{P_E}{P_T} = \frac{R \times V_S}{T \times V_a} = \frac{T(1-t) \times V_S}{T \times V_S(1-w)} = \frac{(1-t)}{(1-w)} \quad (6)$$

where, η_H is Efficiency hull, w is wake fraction, t is thrust deduction fraction,. t and w are propulsor parameter, the value of t is obtained by Equation (7), while w is determined by Equation (8).

$$t = 1 - \frac{R}{T} \quad (7)$$

$$w = 1 - \frac{V_A}{V_S} \quad (8)$$

3.2. Numerical Model

The proposed numerical model by Computational Fluid Dynamics (CFD) for three-dimensional unsteady viscous incompressible flow using ANSYS-CFX software package was developed based on the Reynolds-Averaged Navier-Stokes (RANS) method. In the incompressible flows, the averaged continuity and momentum equation may be given as in the following equation of mass and momentum, equation can be written as in Equations (9) and (10).

$$\frac{\partial \rho}{\partial t} + \nabla.(\rho U) = 0 \quad (9)$$

$$\frac{\partial(\rho U)}{\partial t} + \nabla.(\rho U x U) = -\nabla p + \nabla.\tau + S_M \quad (10)$$

where τ is the stress tensor, is related to strain rate as follow in Equation (11).

$$\tau = \mu(\nabla U + (\nabla U)^T - \frac{2}{3}\delta \nabla.U \quad (11)$$

The total energy equation which is the third governing equation of CFD, the equation can be written as in Equation (12)..

$$\frac{\partial(\rho h_{tot})}{\partial t} - \frac{\partial p}{\partial t} + \nabla.(\rho U h_{tot}) = \nabla(\lambda \nabla T) + \nabla(U.\tau) + U.S_M + S_E \quad (12)$$

where, h_{tot} is the total enthalpy, related to the static enthalpy h, as in Equation (13).

$$h_{tot} = h + \frac{1}{2}U^2 \quad (13)$$

the term $+\nabla(U.\tau)$ is the viscous work term which represents the work due to viscous stress and the term $+U.S_M$ is currently neglected where the term represents the work due to external momentum sources.

Both laminar and turbulent flows without the need of additional information are described in the Navier-Stokes equations. However, at realistic Reynolds number, turbulent flows span a large range of turbulent length and time scales. In produce the Reynolds Averaged Navier-Stokes (RANS) equations, the original unsteady Navier-Stokes equations will be to modify turbulence models seek by introduction of averaged and fluctuating quantities. Because the RANS equation in modeling turbulence is obtained using a statistical average procedure, the RANS equation is called a statistical

turbulent models [20]. The Reynolds Averaged Navier-Stokes (RANS equation as follow in Equations (14) and (15).

$$\frac{\partial \rho}{\partial t} + \frac{\partial}{\partial x_j}\left(\rho U_j\right) = 0 \tag{14}$$

$$\frac{\partial (\rho U)}{\partial t} + \frac{\partial}{\partial x_j}\left(\rho U_i U_j\right) = -\frac{\partial p}{\partial x_j} + \frac{\partial}{\partial x_j}\left(\tau_{ij} - \overline{\rho u_i \rho u_j}\right) + S_M \tag{15}$$

where τ is the moleculer stress tensor (including both normal and sheer the stress component).

The Reynolds stresses is obtained by using the turbulence model in the RANS simulation. In this investigation to evaluate the Reynolds stress tensor using Shear Stress Transport (SST) eddy viscosity model and a Baseline (BSL) Reynolds stress model [21]. The SST model in the inner boundary layer is by blends a variant of the k-ω model and in the outer boundary layer and free stream by blends transformed version of the k-ε model [22]

Transport Equation for Shear Stress Transport (SST) k-ω model as follow in Equation (16) and (17).

$$\frac{\partial}{\partial t}(\rho k) + \frac{\partial}{\partial x_j}(\rho k u_i) = -\frac{\partial}{\partial x_j}\left(\Gamma k \frac{\partial \omega}{\partial x_j}\right) + G\tilde{}k + Yk + Sk \tag{16}$$

$$\frac{\partial}{\partial t}(\rho \omega) + \frac{\partial}{\partial x_j}(\rho \omega u_i) = -\frac{\partial}{\partial x_j}\left(\Gamma \omega \frac{\partial \omega}{\partial x_j}\right) + G\tilde{}\omega - Y\omega + D\omega + S\omega \tag{17}$$

where, $G\tilde{}k$ represents the mean velocity gradients that generates turbulence kinetic energy, $G\tilde{}\omega$ represents the generation of ω, Γk and $\Gamma \omega$ represent the effective diffusivity of k and ω respectively, Sk and $S\omega$ are user-defined source terms, Yk and $Y\omega$ represent the dissipation of k and ω due to turbulence, $D\omega$ represent the cross-diffusion term.

In this simulation, the shear stress transport SST model is applied with a combination of both k-ε and k-ω models, given high accuracy modelling of the boundary layer. Accurate predictions of the on set and the amount of flow separation under opposing pressure gradients where turbulence is present is given by he SST model. To predict good separation by applying both previous models, which covers both regions of the boundary layer, close to the wall and far away from the wall close to the boundary layer limit and applies the Bradshaw relation [23].

4. CFD Analysis of Pre-Duct

4.1. Numerical Simulation

Numerical simulation using CFD is basically the same as other software based computational fluid dynamics; the simulation uses a Fluid Flow Analysis (CFX) solver. The simulation stage uses Ansys R18.2 with several stage: geometry, mesh, pre-processor, solver and post-processor.

The transverse boundaries have been placed suitably, because the width of the domain is infinite, however, doing this in ANSYS CFX or in fact in any CFD Software is not possible. [24]. Based ANSYS recommends for resistance prediction, the velocity inlet of the computational domain should be located at least on ship length upstream from the forward perpendicular, and the velocity outlet at least twice that distance downstream, from the respective perpendicular [21].

The recommendation given by ANSYS that in rare occasions, pressure reflection can occure, this can potentially render the results meaningless of resistance analysis. these concern to these recommendations, the inlet boundary was set 1.5 L ahead of the forward perpendiculars and the pressure outlet 3.5 L downstream from the after perpendicular [25]. the length used in both longitudinal and transverse directions of which was set equal 1.5 L, to eliminate the possibility of a pressure reflection from these boundaries.

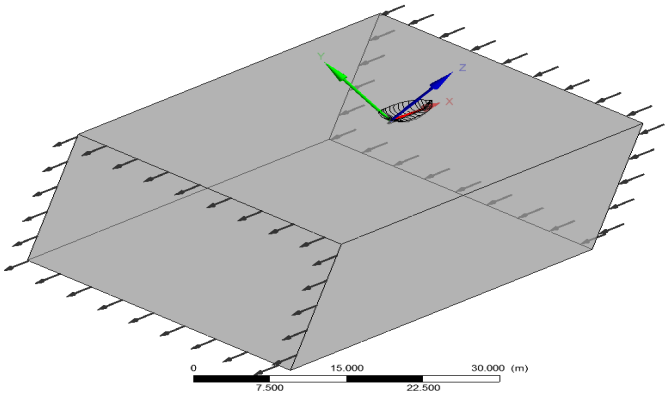

Figure 7. Computational Domain

The CFD software package offer several types of boundary conditions. For the purposes, the boundary in the positive x-direction was set as a velocity inlet, where the flat wave originates, and the negative x-direction was set pressure outlet, which prevents backflow and fixes static pressure at the outlet. Overview of computational domain and boundary condition are illustrated in Figure 7, and Table 3 describes the selected dimension for the fluid domain in the numerical model which represented in ANSYS-CFX.

Table 3. The fluid domain geometry size

Fluid domain entities	Boundary conditions	ITTC	Selected	Distance (m)
Rectangular	Inlet	1–2 L	1.5 L	14.25
	Outlet	3–5 L	3.0 L	24.50
	Top and Bottom wall	1–2 L	1.5 L	14.25
	Side Wall	1–2 L	1.5 L	14.25

4.2. Meshing model

Mesh generation was carried out in the facilities offered on ANSYS CFX. This allows the user to make full use of the software's automatic operations, Firstly, the region-based mesh generated is static in relation to the local coordinate system and therefore to the hull. The prismatic layer mesher was utilised to generate orthogonal prismatic cells next to the hull, the layer mesh allows the software to resolve the near-wall flow accurately as well as capture the effects of flow separation [21]. Resolving these parameters in sufficient detail depends on the flow velocity gradients normal to the wall, which are much steeper in the viscous turbulent boundary layer than would be implied by taking gradients from a coarse mesh. Geometry the model as in Figure 8 and meshing the model as in Figure 9.

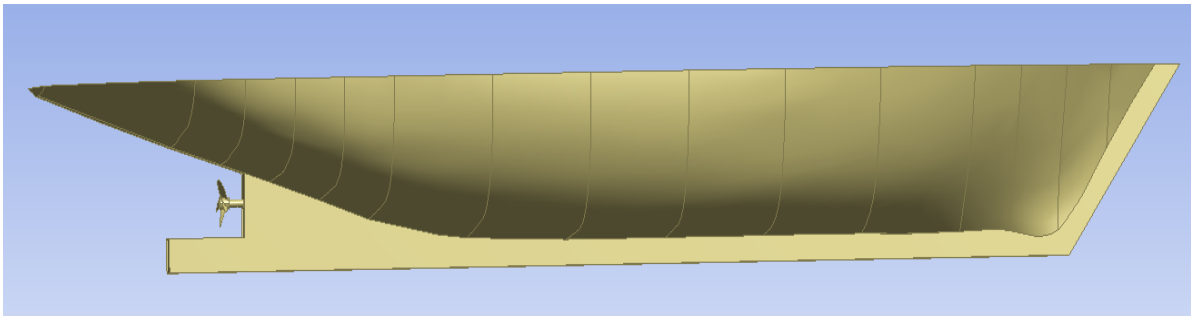

Figure 8. Geometry model

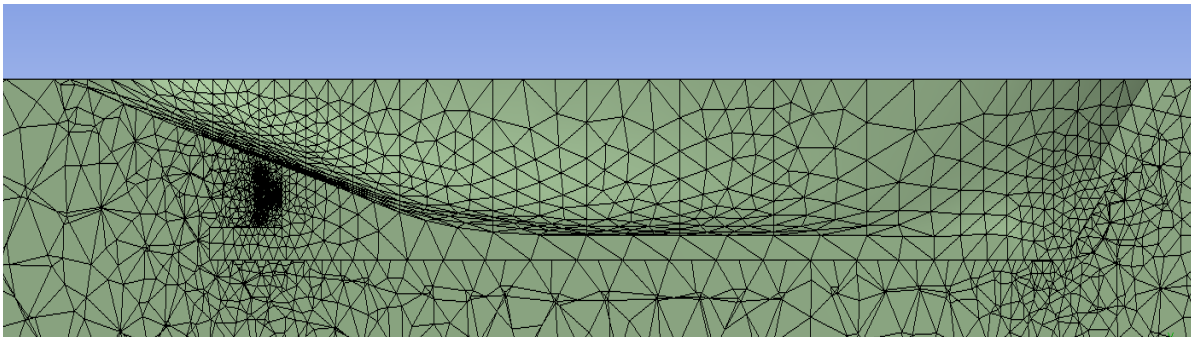

Figure 9. Meshing model

4.3. Pre solver of CFX

To define its analysis method, fluid flow characteristic and its boundary conditions, after the completed mesh model in the previous module is then imported to the Ansys CFX pre solver. The domain characteristic that being applied to the flow, as shown Table 4. And the boundary conditions type that being applied the fluid domain as shown Table 5.

Table 4. Domain characteristics

Criteria	Value
Type of fluid	Water
Density of fluid (kg/m^3)	997
Temperature (^{o} C)	25
Viscosity of kinematic (m^2/s)	8,9 E-7
Morphology	Continuous fluid
Model of buoyancy	Buoyant
Gravity Z component (m/s^2)	-9,81
Domain motion	Stationary
Reference pressure (atm)	1
Model of turbulence	SST
Turbulent wall functions	Standard

Table 5. Boundary condition setting specification

Boundary conditions	Boundary type	Value
Inlet	Inlet	Range of velocity = 1 – 2 [m/s] Model of turbulence : SST model
Outlet	Opening	Momentum and mass : Entrainment Static Pressure: 0 [Pa]
Top, Bottom and Side wall	Walls	Momentum and mass : Free slip wall
Hull	Walls	No Slip wall

4.4. Convergence and Grid Independence

Convergence is defined as determining the number of iterations and Root Means Square (RMS) limits before the flow solver phase of the CFD is carried out, which is the stage of determining boundary conditions that must be applied to the simulation process. The number of iterations used affects the

amount of time in the simulation process, the more iterations the more time it takes. The number of iterations needed is directly proportional to the number of elements used in the modeling process. The magnitude of the convergent value limit or the RMS limit used in modeling related to fluid behavior is 10^{-5}, the value is the best convergence value and has been widely used in engineering applications [21]. Convergence simulation as in Figure 10.

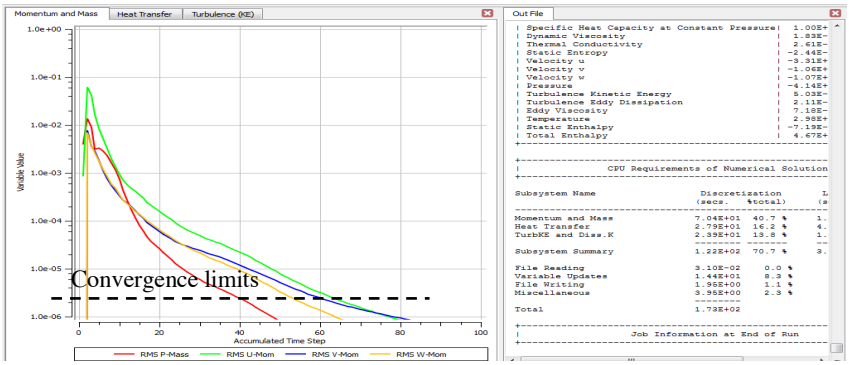

Figure 10. Convergence of iteration processes

Grid modeling uses un-uniform approach in which each element will have a different size. a uniform grid will help to define the model in critical areas, especially in parts that have a sharp bend, the size of the grid will be smaller and much in the critical area, this is related to the quality of the grid used and the convergence and accuracy of the simulations performed [26]. Grid independence is one of the main principle of the accuracy of the results of CFD simulations, grid independence for modeling done as in Figure 11.

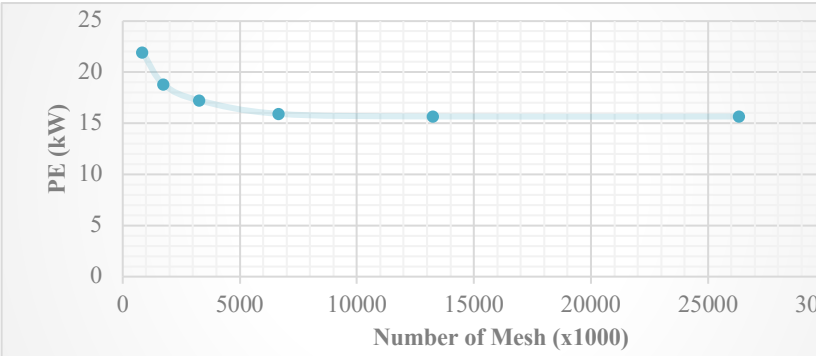

Figure 11. Grid independence

4.5. Validation of Pre-Duct computation

Validation is an attempt to show the level of truth of the modeling simulation conducted. Holtrop method on Maxsuf Resistance is a method used to determine the ship's resistance single screw propeller to: tankers, general cargo, fishing vessels, tugboats, container and frigate [27], Validation of CFD modeling simulations for traditional fishing vessels that apply pre-duct by comparing the results of modeling simulations using Maxsurf Resistance (Holtrop Method). Figure 12 shows the results of a fishing vessel modeling simulation with CFD and modeling simulation Maxsurf Resistance (Holtrop Method), and calculation of total ship resistance obtined from CFD modeling simulation and Masurf Resistance modeling simulation has the same trend, the Holtrop method has a greater value of 14%.

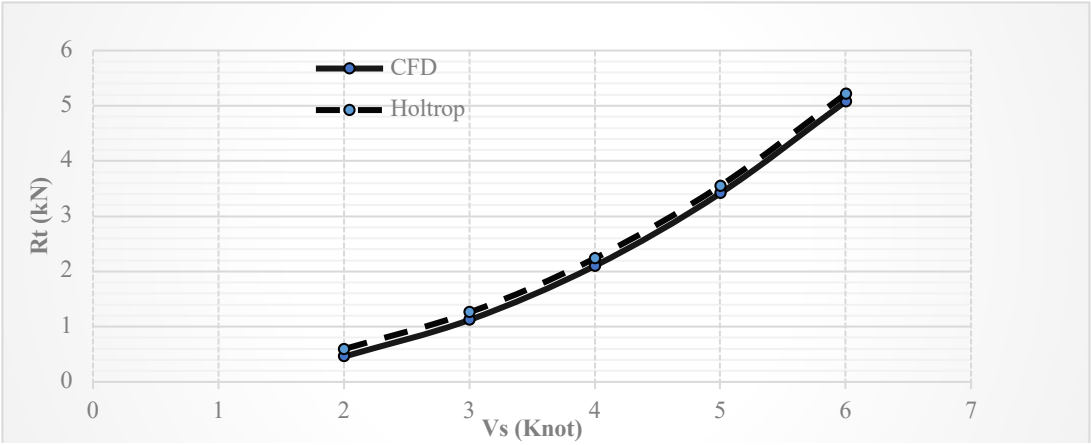

Figure 12. Comparison of the ship resistance by CFD and Holtrop method

4.6. Result of Pre-Duct computations

The results of computation of propulsor performance for the ship with and without pre—duct are shown in Figure 13 and Table 6-8. The application of pre-duct on traditional fishing vessels increases the resistance of the ship, but it can increase propulsor performance to be higher, so the engine power requirements can be reduced by 2.8% for pre-duct with a 10 degree rake angle. This increase in performance is due to the duct that pre-duct can direct the flow of fluid towards the propeller

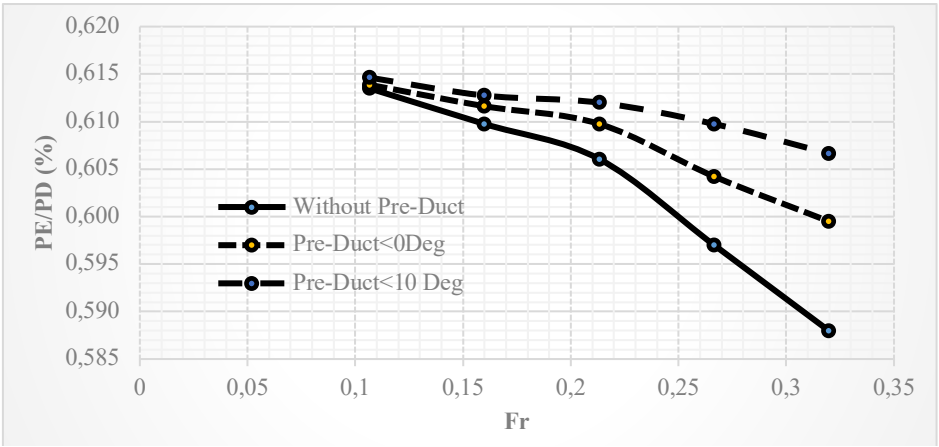

Figure 13. Comparison PE/PD with and without Pre-Duct

Table 6. Model result with and without Pre-Duct

Fr	Without Pre-Duct		Pre-Duct (α = 0 degree)		Pre-Duct (α = 10 degree)	
	P_E (kW)	P_D (kW)	P_E (kW)	P_D (kW)	P_E (kW)	P_D (kW)
0.106	0.47	0.77	0.47	0.76	0.47	0.76
0.159	1.73	2.84	1.73	2.83	1.73	2.82
0.213	4.32	7.13	4.31	7.07	4.31	7.04
0.266	8.78	14.71	8.76	14.50	8.76	14.37
0.319	15.67	26.65	15.70	26.19	15.70	25.89

Table 7. Model result in speed 6 knot and rake angle of duct 0 deg.

Condition	P_E (kW)	w	t	P_D (kW)
Bare hull (without duct)	15.670	0.195	0.117	26.650
With Pre-Duct (α = 0 degree)	15.701	0.278	0.143	26.190
Difference	0.198%	0.083	0.026	-1.726%

Table 8. Model result in speed 6 knot and rake angle of duct 10 deg.

Condition	P_E (kW)	w	t	P_D (kW)
Bare hull (without duct)	15.670	0.195	0.117	26.650
With Pre-Duct (α = 10 degree)	15.706	0.286	0.135	25.890
Difference	0.230%	0.091	0.018	-2.852%

CFD modeling simulation results show that the wake factor (1-w) decreased, a decrease that occurs by 0.083 at pre-duct with rake angle 0 degree and without pre-duct as in the Table 7, in the pre-duct with rake angle 10 degree there was a decrease of 0.091 as in the Table 8, a decrease in wake factor is caused by reflecting flow generated form pre-duct. In addition to the thrust deduction factor (1-t) as in the Table 7 and 8 there was a decrease but it was not significant, thus the efficiency of hull (η_H) equation (6) at a shop speed of 6 knots, an increase occurs as shown in Figure 14.

From the results of modeling simulations, at a speed of 6 knots, the resistance of fishing vessels with and without pre-duct as shown in Figure 15, which shows that the resistance of the fishing vessels increased. The increase is caused by the addition of the device to the hull ship, while the angle formed by the profile of pre-duct also increases the ship's resistance. The increase in ship resistance on a fishing vessel that occurs is followed by an increase in thrust efficiency as illustrated in Figure 13, which shows an increase in the thrust efficiency of the fishing vessel.

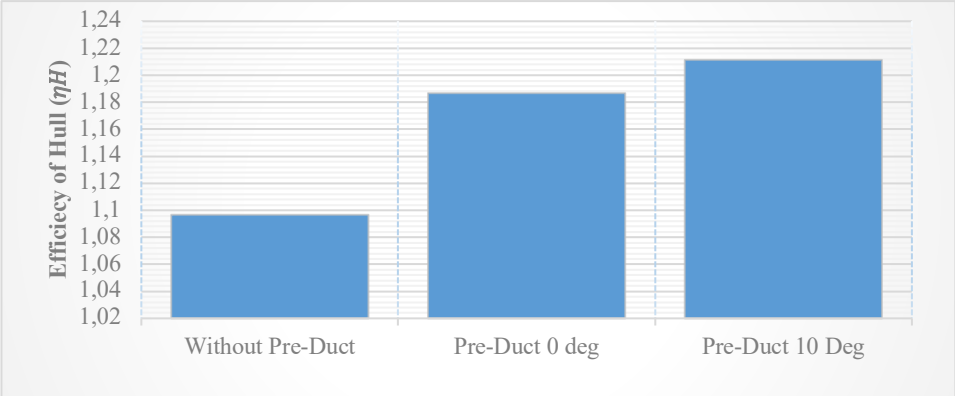

Figure 14. Efficiency of Hull with and without Pre-Duct

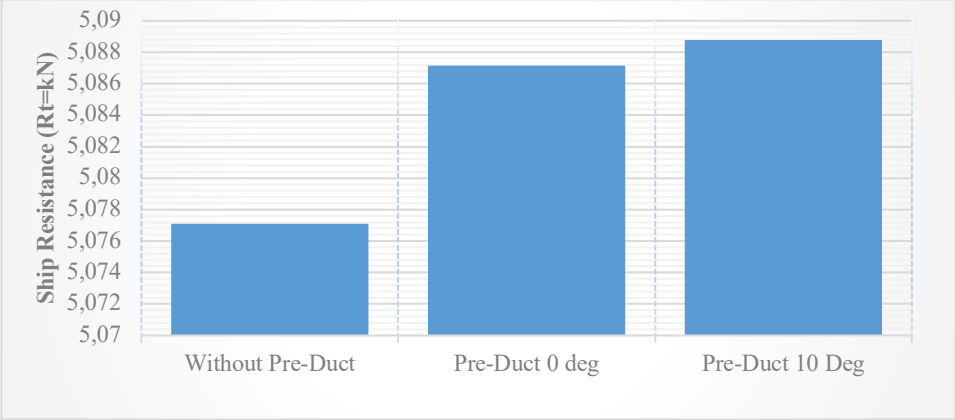

Figure 15. Ship Resistance with and without Pre-Duct

The increased efficiency that occurs due to the use of pre-ducts on fishing vessels is caused to several things including:

1. Generation of thrust by the profile of duct, there is a strong downflow along the stren hull, it is possible to make the duct generate thrust by using a suitable duct attack angle and blade shape.
2. Increase in wake gain, the duct reduces the velocity of the flow behind it, it is possible to increase wake gain by guiding this slower flow to the propeller blade.

5. Conclusion

CFD method has been used to analyse the benefit use of ESD such as the implementation of pre-duct on a traditional (Lamongan base) fishing vessel with quite successful results. It is apparent that the use of pre-duct on traditional fishing vessels has an increase of ship resistance $\pm$0.2%, but the increase of ships resistance is complemented by an increase in the performance of ship propulsion system about 1.7% on vessels with pre-duct at rake angle 0^o, while 2.8% on vessels with pre-duct at rake angle 10^o. Implementation pre-duct increased efficiency energy and improving ship propulsion performance $\pm$3%.

References

[1] Ø. Buhaug *et al.*, Eds., *Second IMO GHG Study 2009*. London: International Maritime Organization, 2009.
[2] S. A. Harvald, *Resistance and Propulsion of Ships*. United States of America: John Wiley & Sons, Inc, 1983.
[3] A. F. Molland, S. R. Turnock, and D. A. Hudson, *Ship resistance and propulsion*. United States of America: Cambridge University Press 32 Avenue of the Americas, New York, NY 10013-2473, USA, 2011.
[4] C. Jinjun, W. Chengsheng, P. Ziying, and Z. Wentao, "Evaluation for A Sail-assisted Bulk Carrier Operating on The Route of Hong Kong - Yokohama," in *Greenship Procedings 2011*, 2011.
[5] J. S. Carlton, "Thrust Augmentation Devices," *Mar. Propellers Propuls.*, no. 1986, pp. 367–378, 2019.
[6] F. Mewis, "A Novel Power-Saving Device for Full-Form Vessels," *First Int. Symp. Mar. Propulsors*, no. June, 2009.
[7] F. Mewis and T. Guiard, "Mewis Duct ® – New Developments , Solutions and Conclusions," in *Second international symposium on Marine Propulsors*, 2011, no. June, pp. 1–8.
[8] J. Dang, H. Chen, D. Guoxiang, A. Van Der Ploeg, R. Hallmann, and F. Mauro, "An Exploratory Study on the Working Principles of Energy Saving Devices (ESDs)," *Symp. Green Sh. Technol.*, no. October, 2011.

[9] J. Dang, G. Dong, and H. Chen, "An Exploratory Study on The Working Principles of Energy Saving Devices (ESDS) - PIV, CFD Investigations and ESD Design Guidelines," in *Proceedings of the ASME 2012 31st International Conference on Ocean, Offshore and Arctic Engineering OMAE2012*, 2012, pp. 1–10.
[10] H. J. Shin, J. S. Lee, K. H. Lee, M. R. Han, E. B. Hur, and S. C. Shin, "Numerical and experimental investigation of conventional and un-conventional preswirl duct for VLCC," *Int. J. Nav. Archit. Ocean Eng.*, vol. 5, no. 3, pp. 414–430, 2013.
[11] N. Nomura and T. Yamazaki, *Fishing Techniques*. Tokyo: Japan International Coorperation Agency, 1975.
[12] A. Permana and R. Awwalin, "The Influence of Hull Forms of Traditional Fishing Vessels in Brondong Coast to Ship's Resistance," *Baita Eng. J. Nav. Archit. Mar. Eng.*, vol. 1, no. 1, pp. 47–58, 2019 (Article in Bahasa Indonesia).
[13] A. Permana, A. Munazid, B. Suwasono, and R. Awwalin, "The Influence of Ship Particulras to Resistance of Fishing Vessles 5 GT in The Brondong Lamongan Coast," in *Prosiding Seminar Nasional Kelautan ke XIII*, 2018, pp. 60–68 (Article in Bahasa Indonesia).
[14] K. Rohmad and A. Munazid, "Technical Characteristics Hull Forms of Traditional Fishing Vessels in Paciran Lamongan Coast," in *Prosiding Seminar Nasional Kelautan ke XIII*, 2018, pp. 69–77 (Article in Bahasa Indonesia).
[15] A. F. Molland, S. R. Turnock, D. A. Hudson, and I. K. A. P. Utama, "Reducing ship emissions: A review of potential practical improvements in the propulsive efficiency of future ships," *Trans. R. Inst. Nav. Archit. Part A Int. J. Marit. Eng.*, vol. 156, no. PART A2, pp. 175–188, 2014.
[16] G. Dyne, "The Efficiency of a Propeller in Uniform Flow," *Trans. R. Inst. Nav. Archit. Part A Int. J. Marit. Eng.*, vol. 13, 1994.
[17] G. Dyne, "The Principles of Propulsion Optimisation," *Trans. R. Inst. Nav. Archit. Part A Int. J. Marit. Eng.*, vol. 137, 1995.
[18] J. Carlton, *Marine Propellers and Propulsion*, 4th ed. Butterworth-Heinemann is an imprint of Elsevier, 2018.
[19] F. Joel H. and P. Milovan, *Computational Methods for Fluid Dynamics*, Third, Rev. New York, 2002.
[20] J. John D. Anderson, *Computational Fluid Dynamics: The Basics with Applications*, vol. 332, no. 7555. New York, United States of America, 1995.
[21] T. D. Canonsburg, *ANSYS CFX-Solver Modeling Guide*, vol. 15317, no. November. United States of America, 2011.
[22] F. R. Menter, "Two-Equation Eddy-Viscosity Turbulence Models for Engineering Applications," *AIAA J.*, vol. 32, no. 8, 1994.
[23] F. R. Meter, M. Kuntz, and R. Langtry, "Ten Years of Industrial Exxperience with the SST Turbulence Model," *Turbul. Heat Mass Transf. 4*, 2003.
[24] F. B. Robert, N. J. Nicholas, and T. E. O., "Hydrodynamic Forces on Ships id Dredged Channels," 1974.
[25] A. G. Elkafas, M. M. Elgohary, and A. E. Zeid, "Numerical study on the hydrodynamic drag force of a container ship model," *Alexandria Eng. J.*, vol. 58, no. 3, pp. 849–859, 2019.
[26] R. Deng, D. bo Huang, J. Li, X. kai Cheng, and L. Yu, "Discussion of grid generation for catamaran resistance calculation," *J. Mar. Sci. Appl.*, vol. 9, no. 2, pp. 187–191, 2010.
[27] J. Holtrop and G. Mennen, "A statistical power prediction method," *Int. Shipbuild. Prog.*, vol. 25, no. 290, pp. 253–256, 1978.